Analytic Ray Tracing for the Study of HF Magneto-ionic Radio Propagation in the Ionosphere

J. A. Bennett
Department of Electrical and Computer Systems Engineering
Monash University, Clayton, Vic., Australia 3168

J. Chen, P. L. Dyson
Department of Physics, Latrobe University, Bundoora, Vic., Australia 3083

Abstract

Ray tracing provides a quantitative tool for the study of HF radio wave propagation in the ionosphere, but its use is limited in many applications by the time required to numerically trace many separate rays. One approach to overcoming this problem is the use of ionospheric models that admit analytic solutions of the ray tracing equations. Such a model may be based on a vertical plasma frequency profile consisting of what are known as quasi-parabolic segments. Analytic tracing is much faster than numerical tracing (from 5 to 10 times), but more limited in the range of situations that can be considered.

The main thrust of the paper is to present and test a technique, based on the use of an equivalent operating frequency, that allows the analytic results to be extended to take approximate account of the magneto-ionic effects associated with the earth's magnetic field. Errors in group path, phase path and ground range are generally less than 5 km, errors in absorption generally less than 5%.

1. Introduction

1.1 Ray tracing in the ionosphere

Ray tracing provides a quantitative tool for the study of HF radio wave propagation in the ionosphere. The validity of the ray approach rests on the medium changing slowly on the scale of the wavelength. Even when this condition is not strictly met, ray tracing often gives qualitatively correct results. However, it does need to be born in mind that there are occasions when the gradients present are sufficient to invalidate the ray picture. There is not sufficient space here to discuss the full significance of the ray construction in terms of quasi-optics and the progressive wave formalism introduced by Lewis [1965].

To radio waves, the ionosphere appears as an inhomogeneous and anisotropic medium, the properties of which are affected by the earth's magnetic field. Interest in the use of general ray tracing for HF waves in the ionosphere can be followed from the early work of Booker [1936] and Poeverlein [1948]. The widespread availability of powerful high speed digital computers has made numerical ray tracing in the ionosphere a practical proposition. Interest in ionospheric ray tracing was stimulated by the papers of Haselgrove [1955] and Haselgrove & Haselgrove [1960] who went back to the work of Hamilton first published in 1837 [Conway and Synge 1931], as indeed had Poeverlein [1948].

By far the most widely distributed general ray tracing program for HF waves in the ionosphere is that of Jones [1966,1968]. It is still in use in many places, despite the fact that a number of researchers have continued to develop new ray tracing programs. The program lacks two important features, automatic homing-in and field strength calculations. An account of recent trends in ionospheric ray tracing has been given by Bennett *et al.* [1990].

The main factor limiting the use of ray tracing in many applications is the time required. It is frequently necessary to trace many separate rays and numerical ray tracing is slow. One approach to overcoming this problem, the one considered in this

paper, is the use of analytic ray tracing. It is much faster, but it is more restricted in the situations to which it can be applied.

1.2 Analytic ray tracing

Croft and Hoogasian [1968] showed that exact ray solutions can be obtained for a spherical ionosphere using a quasi-parabolic ionospheric model, if the effect of the earth's magnetic field is neglected. Later Hill [1979] modelled a more complicated ionosphere using several distinct quasi-parabolic and quasi-linear [Westover 1968] layers. Milsom [1985] fitted a combination of quasi-linear and quasi-parabolic layers to the CCIR model. Dyson and Bennett [1988] and Baker and Lambert [1989] have independently demonstrated the advantages of a model consisting of smoothly joined quasi-parabolic layers or segments in the study of oblique radio wave propagation in the ionosphere. Baker and Lambert [1989] have discussed the use of such a model in single-station location of distant radio transmitters, while Dyson and Bennett [1991] have shown how the model can be generalized by including a tilt.

Chen, *et al.* [1990] introduced a quasi-parabolic segment (QPS) model. It makes use of a number of quasi-parabolic segments (typically from 1 to 15) and a quasi-linear base segment. It can represent any number of layers and valleys in the ionosphere, and describe accurately a wide variety of ionospheric profiles. Chen, *et al.* [1990] showed that the parameters of the model can be determined automatically by fitting to actual data points. In the absence of the earth's magnetic field, this model can give analytic expressions for ground range, group path, phase path, loss of signal strength due to ray spreading, and so on, for oblique radio propagation. The expressions obtained are free of the spurious singularities that arise with models made up of segments that are not joined up smoothly [Milsom 1985].

There are two main limitations on the usefulness of the analytic results described. First, only a very limited class of horizontal gradients can be included. Second, the effect of the earth's magnetic field on the propagation, that is magneto-ionic effects, are not included. It is the second limitation that is addressed in this paper.

It is true that for short paths not lying in the magnetic meridian, the no-field results can be taken as representative of the ordinary mode results. Also by the use of a frequency scaling technique, Chen *et al.* [1990] have shown how approximate results can be obtained also for the path of the extraordinary mode. This approach is examined more systematically here, and extended to the case of absorption.

1.3 Approximate allowance for magneto-ionic effects

As discussed in the appendix, the method of allowing for the effect on the earth's magnetic field on the radio propagation is based on the use of an equivalent operating frequency. Ideally, this would be the frequency which leads to the same results in the absence of the magnetic field as those applying at the actual frequency when the field is present. In general, there is no exact equivalent frequency in this sense. However, it is shown that for a wide range of conditions approximate equivalent frequencies exist, and the same approximate equivalent frequency applies to such quantities as ground range and phase path for a given initial elevation angle of the ray.

In the case of both group path and absorption, the same approximate equivalent frequency may be used if an additional correction term is included. (Phase path, group path and absorption are defined in the next section.)

1.4 Organization of the remainder of the paper

In Section 2 the equations governing radio ray tracing in the ionosphere are presented. These equations are the basis of a numerical ray tracing program against which the approximate analytic results are checked. In Section 2.2 it is shown how the ray equations lead to analytic results for a spherically symmetric ionosphere in which the radial dependence of electron plasma frequency is governed by the quasi-parabolic function.

In this paper, for the first time, the analytic results are extended to include absorption of energy in the ionosphere due to particle collision. To make a realistic study of this phenomenon which is most important during day light hours, it is necessary to include the D region of the ionosphere. In the D

region, the plasma frequency is an approximately exponential function of radius. The method of obtaining analytic ray tracing results for this region of the ionosphere is less elegant than that applied to higher layers and it leads to an approximate doubling of the computer time required.

In Section 3 the ionospheric model used to test the approximate analytic results is set up. The same general method can be employed to set up models applying in particular circumstances.

In Section 4 the analytic results applying to the ionospheric model are obtained. Finally, in Section 5 representative results are presented graphically and compared with the results of numerical ray tracing.

2. Equations of Ionospheric Ray Tracing

2.1 General equations

The Hamiltonian ray equations, written in spherical co-ordinates and using physical components of the wave propagation vector, can be written in the form

$$\frac{dr}{du} = \frac{1}{\mu\mu'}\left(V_r - \frac{1}{2}\frac{\partial\mu^2}{\partial V_r}\right) \tag{1}$$

$$\frac{d\theta}{du} = \frac{1}{\mu\mu' r}\left(V_\theta - \frac{1}{2}\frac{\partial\mu^2}{\partial V_\theta}\right) \tag{2}$$

$$\frac{d\phi}{du} = \frac{1}{\mu\mu' r\sin\theta}\left(V_\phi - \frac{1}{2}\frac{\partial\mu^2}{\partial V_\phi}\right) \tag{3}$$

$$\frac{dV_r}{du} = \frac{1}{2\mu\mu'}\frac{\partial\mu^2}{\partial r} + V_\theta\frac{d\theta}{du} + V_\phi\sin\theta\frac{d\phi}{du} \tag{4}$$

$$\frac{dV_\theta}{du} = \frac{1}{r}\left(\frac{1}{2\mu\mu'}\frac{\partial\mu^2}{\partial\theta} - V_\theta\frac{dr}{du} + rV_\phi\cos\theta\frac{d\phi}{du}\right) \tag{5}$$

$$\frac{dV_\phi}{du} = \frac{1}{r\sin\theta}\left(\frac{1}{2\mu\mu'}\frac{\partial\mu^2}{\partial\phi} - V_\phi\sin\theta\frac{dr}{du} - rV_\phi\cos\theta\frac{d\theta}{du}\right) \tag{6}$$

where r, θ and ϕ are the spherical polar coordinates of a point on the ray path, V_r, V_θ and V_ϕ are physical components of a vector of magnitude μ in the wave normal direction, and μ and μ' are the phase and group refractive indices. The independent variable u has been taken as elapsed group path along the ray.

These equations are widely known in the ionospheric literature as Haselgrove's equations, following the work of Haselgrove [1955]. The name group path, for a distance equivalent to the time of flight of a pulse, was introduced by Appleton [1928]. It is commonly denoted P'. The relative slowness, in the sense introduced by Synge [1954], is not μ' but $\mu'\cos\alpha$, where α is the angle between the ray direction and ($\underline{V}$), the direction of phase propagation. Corresponding to group path which refers to the time of pulse propagation, the phase path, denoted P, represents the time of phase propagation. For the case of point sources (mostly adequate for the study of ionospheric radio), P is proportional to the eikonal function. The phase path is given by

$$\frac{dP}{du} = \frac{\mu}{\mu'} \tag{7}$$

and the absorption by [Bennett and Dyson 1978]

$$\frac{dA}{du} = \frac{1}{2}\frac{\omega}{c}\frac{Z}{(1+g)}\frac{(\mu'-\mu)}{\mu'} \tag{8}$$

where the normalized electron collision frequency Z is defined below. A is the absorption in nepers. The absorption in decibels is $8.686A$.

The refractive index is given as the Appleton-Lassen formula, [*e.g.* Budden 1966]

$$\mu^2 = 1 - \frac{X}{1 - [Y_T^2/2(1-X)] \pm \sqrt{[Y_T^4/4(1-X)^2] + Y_L^2}} \tag{9}$$

where the normalized variables are given by

$$\begin{aligned} X &= \frac{e^2 N}{\varepsilon_0 m\omega^2} = \frac{f_N^2}{f^2} \\ Y &= \frac{e B_0}{m\omega} = \frac{f_H}{f} \\ Y_L &= \frac{e B_L}{m\omega} \\ Y_T &= \frac{e B_T}{m\omega} \\ Z &= \frac{\nu}{\omega} = \frac{\nu/2\pi}{f}. \end{aligned} \tag{10}$$

Here N is the electron concentration, $B_0$the earth's magnetic field, and ν an appropriate average electron collision frequency. All these variables depend

upon position in the earth's ionosphere. Further,

$$\begin{aligned} B_L &= B_0 \cos\Theta \\ B_T &= B_0 \sin\Theta \end{aligned} \tag{11}$$

and where Θ is the angle between the direction of phase propagation and the direction of the magnetic field. The subscripts T and L refer to the transverse and longitudinal components of the imposed magnetic field with reference to the direction of the wave normal.

The positive sign (+) and negative sign (−) in (9) make the refractive index two valued. Two modes exist, known as the ordinary mode and the extraordinary mode.

The $\partial\mu^2/\partial V$ terms in the ray equations arise from the Θ dependence of μ^2. Note that

$$V_r^2 + V_\theta^2 + V_\phi^2 = \mu^2. \tag{12}$$

In the absence of an imposed magnetic field ($Y_T = Y_L = 0$), the refractive index takes a much simpler form.

The group refractive index is defined by

$$\mu' = \frac{\partial(\omega\mu)}{\partial\omega}. \tag{13}$$

The quantity g occurring in (8) can be written

$$g = \frac{1}{2} Y h \tag{14}$$

where h depends upon Θ and upon X and Y only in the combination $Y/(1-X)$. Curves of h were given by Dyson and Bennett [1980], and are shown in Figure 1. It can be seen that h always lies between -1 and 1. Useful approximations apply in a number of cases. For example, for the ordinary mode with $X = 1$, $h = 0$, while for the extraordinary mode with $X = 1 - Y$, $h = -1$.

In this paper, the Hamiltonian ray equations are only used in the case when $\partial\mu^2/\partial\theta$ and $\partial\mu^2/\partial\phi$ are zero.

2.2 Analytic results neglecting the earth's magnetic field

When $Y_L = Y_T = 0$,

$$\mu^2 = 1 - X \tag{15}$$

and

$$\mu\,\mu' = 1. \tag{16}$$

Since μ is now isotropic, and the ionosphere is spherically stratified, we may choose ray propagating in the meridian plane. Hence $V_\phi = 0$ and $\partial\mu^2/\partial\theta = 0$. Therefore from (5),

$$r\frac{dV_\theta}{du} + V_\theta \frac{dr}{du} = 0 \tag{17}$$

so that rV_θ is constant along a ray. Thus

$$V_\theta = \frac{r_0}{r} \cos\beta_0 \tag{18}$$

where r_0 is the earth's radius and β_0 the initial elevation angle of the ray. Rather than making use of (4), from (12) it follows that

$$V_r = \pm\sqrt{\mu^2 - (\tfrac{r_0}{r})^2 \cos^2\beta_0}. \tag{19}$$

The (+) sign applies on the upward section of the ray and where reflection occurs, the (−) sign applies on the downward section of the ray.

From (1),

$$\frac{dr}{du} = \pm\sqrt{\mu^2 - (\tfrac{r_0}{r})^2 \cos^2\beta_0}. \tag{20}$$

Reflection occurs at $r = r_t$, if

$$\mu^2 - (\tfrac{r_0}{r_t})^2 \cos^2\beta_0 = 0. \tag{21}$$

The expression for dr/du enables integrals for various ray quantities to be written in terms of r. From (20), the group path can be written

$$P' = 2\int_{r_0}^{r_t} \frac{r\,dr}{\sqrt{r^2\mu^2 - r_0^2\cos^2\beta_0}}. \tag{22}$$

The factor 2 arises from the up and down sections of the ray.

From (7) and (20), the phase path can be written

$$P = 2\int_{r_0}^{r_t} \frac{r\mu^2\,dr}{\sqrt{r^2\mu^2 - r_0^2\cos^2\beta_0}}. \tag{23}$$

From (2), (18) and (20), the ground range can be written

$$D = 2\,r_0^2\cos\beta_0 \int_{r_0}^{r_t} \frac{dr}{r\sqrt{r^2\mu^2 - r_0^2\cos^2\beta_0}} \tag{24}$$

where

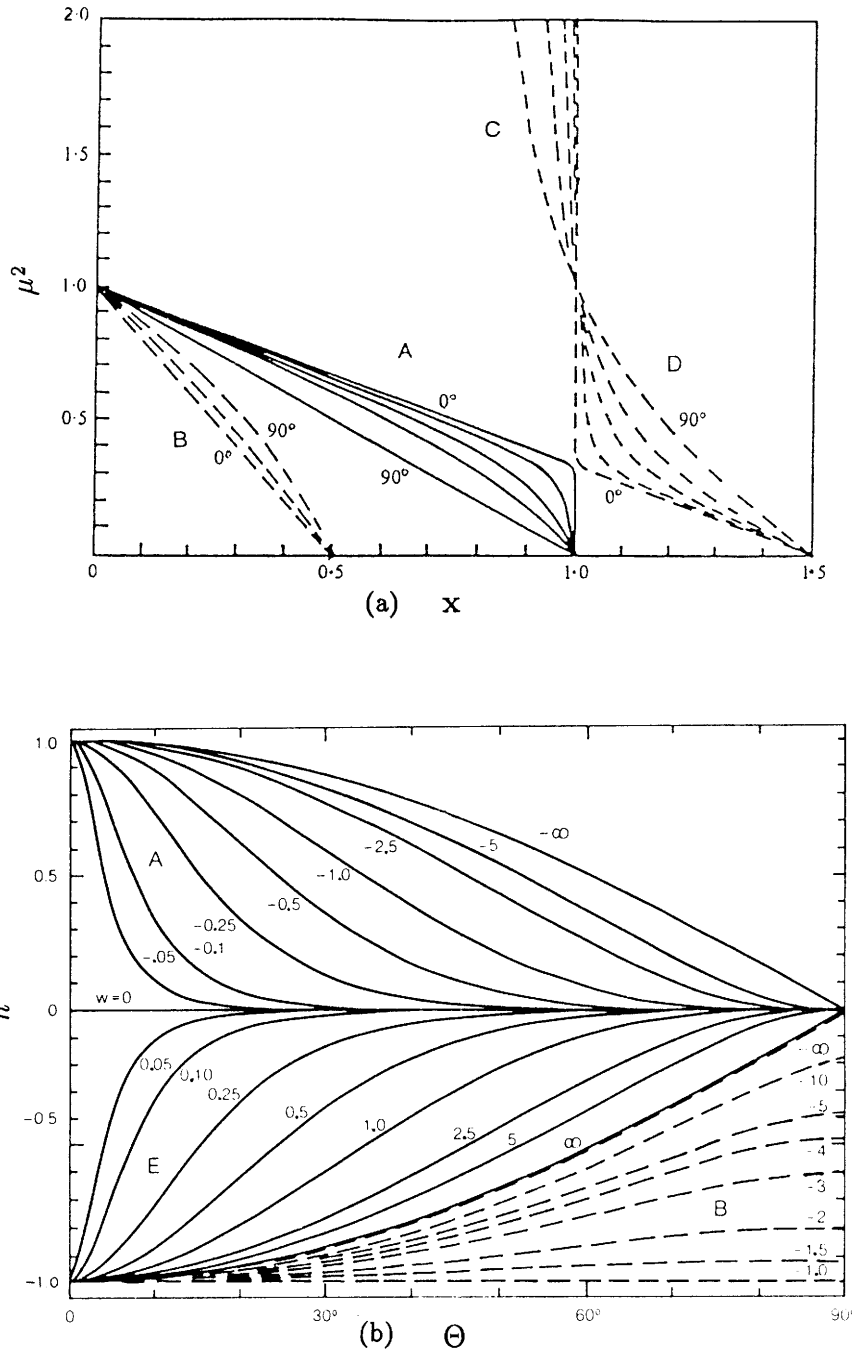

Figure 1: (a) The square of the refractive index as given by the Appleton-Lassen formula for the case $Y = 1/2$. (b) The function h. The matching regions A and B of the diagrams are relevant to the present study.

β_0 is the initial elevation angle at the surface of the earth,
r_0 is the earth's radius,
r_t is the radial distance at which the ray is reflected,
r is the radial distance of the ray at any point, and
μ is the refractive index.

In the quasi-parabolic function introduced by Croft and Hoogasian [1968] to represent ionospheric layers, the plasma frequency f_N is given by

$$f_N^2 = \begin{cases} f_P^2[1 \mp (\frac{r-r_m}{y_m})^2(\frac{r_b}{r})^2] & \text{if } r_b < r < \frac{r_m r_b}{r_b - y_m} \\ 0 & \text{otherwise} \end{cases} \quad (25)$$

where

f_P is the peak value of the plasma frequency,
r_b is the radial distance at the base ionosphere,
r_m is the value of r where $f_N = f_P$, and
$y_m = r_m - r_b$, is the layer semithickness.
The plus (minus) sign in the equation means that the plasma frequency has a maximum (minimum) value at $r = r_m$.

Croft and Hoogasian [1968] employed the (−) sign. This function has the advantage that it is very like the parabolic function used in much ionospheric modelling, while at the same time causing the integrals to take a form possessing analytic results. Complex ionosphere profiles can be built up using a combination of these functions as discussed in Section 1.2. These modes also possess analytic solutions.

3. Ionospheric model

3.1 Model of the plasma frequency

The approximate equations for absorption are of particular interest, and it is a more stringent test of these to consider frequencies reflected from the E layer of the ionosphere which are generally lower than those reflected from the F layer. Thus the ionospheric model used in this study includes a single quasi-parabolic layer with peak height corresponding to the normal E region. In order to examine absorption, the D region is represented by an exponential tail with IRI parameters [Rawer 1981], and another quasi-parabolic layer is used to join the D and E regions. To describe the whole ionosphere smoothly, at the point where this joining layer joins with D region, both the square of the plasma frequency, f_N^2, and its gradient are matched. Similarly, at the joining point with the E layer, both f_N^2 and its gradient are matched. Thus this joining point can be determined automatically.

The quasi-parabolic function is given in (25), and it can be further expressed as

$$f_N^2 = \frac{A}{r^2} + \frac{B}{r} + C \quad (26)$$

where

$$\begin{aligned} A &= \mp f_N^2 r_m^2 \frac{r_b^2}{y_m^2} \\ B &= \pm 2 f_P^2 r_m \frac{r_b^2}{y_m^2} \\ C &= f_P^2 \mp f_P^2 \frac{r_b^2}{y_m^2} \end{aligned} \quad (27)$$

The parameters A, B and C for the E layer are determined by fitting to IRI data [Rawer 1981] using the same technique as described by Chen *et al.* [1990]. The parameters for the joining layer are determined automatically by the conditions mentioned before.

The exponential tail for the D region is obtained using the IRI model [Rawer 1981], and is a third degree polynomial centered at the inflection point to approximate the logarithm of the density. It may be written as

$$N_e = N_{MD} \exp(F_{P1}\, x + F_{P2}\, x^2 + F_{P3}\, x^3) \quad (28)$$

where

$$x = r - r_{MD}$$

and r_{MD}, N_{MD} are the radial distance and electron density at the inflection point.

Since r_{MD} is at an inflection point of the electron density the second derivative is zero, and from (28),

$$F_{P2} = -\frac{F_{P1}^2}{2}. \quad (29)$$

It is also found that F_{P1} is the logarithmic derivative at the height r_{MD},

$$F_{P1} = \frac{d\ln(N_e)}{dr} \qquad (r = r_{MD}). \quad (30)$$

Table 1: The IRI data for the D and E regions ($LATI$ = 35.7°, $LONGI$ = 140.0°, R = 10, $MONTH$ = 3, $HOUR$ = 12.0, $MLAT$ = 25.6°, h_{MD} = 81km, $N_{MD} = 5.69 \times 10^8 \mathrm{m}^{-3}$, h_{ME} = 110km, $N_{ME} = 1.24 \times 10^{11} \mathrm{m}^{-3}$).

h(km)	$N_e(\mathrm{m}^{-3})$	f_N(MHz)
80.0	5.426×10^8	0.209
85.0	1.123×10^9	0.301
90.0	1.182×10^{10}	0.975
95.0	4.818×10^{10}	1.969
100.0	9.550×10^{10}	2.773
105.0	1.206×10^{11}	3.116
110.0	1.241×10^{11}	3.161

Finally, F_{P3} can be expressed in terms of a scale height H which is the height difference between r_{MD} and the radial distance where the electron density has dropped to N_{MD}/e.

$$F_{P3} = (F_{P1}^2 \times H^2/2 - F_{P1} \times H - 1)/H^3 \quad (31)$$

Because the gradient above r_{MD} is much greater than it is below r_{MD}, there are a different scale height, H_a, and a different F_{P3a} above r_{MD}. It follows that

$$F_{P3a} = (F_{P1}^2 \times H_a^2/2 - F_{P1} \times H_a + 1)/H_a^3. \quad (32)$$

Values for all these parameters can be found in the IRI report [Rawer 1981] for different time, geographic location and sunspot activity.

The sample data used in this work are listed in Table 1, and the corresponding fitted ionosphere is shown in Figure 2. The fit to the lower part of the E region could be improved by using several QPS segments as discussed by Chen *et al.* [1990]. However this is unnecessary here since what is important is that the profile be realistic, not a perfect fit to the IRI.

3.2 The collision frequency profile

The subject of collisions between particles in a plasma is complicated. Any collision frequency is a statistical average with respect to the velocities of the colliding particles and the directions of their paths before and after the collision. In a full theory it is found that in different applications, this average must be taken in different ways, so that many different collision frequencies have to be defined.

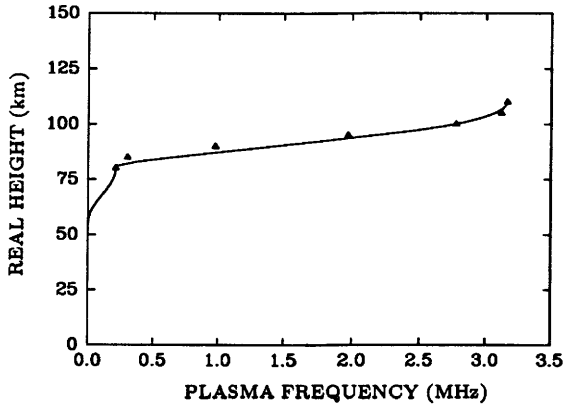

Figure 2: Fitted ionospheric profile with two quasi-parabolic segments and an exponential tail corresponding to the data listed in Table 1.

Since no direct measurements of collision frequency with respect to height were available at the locations considered in this work, the model of the electron collision frequency profile discussed by Ferguson and McNamara [1986] has been adopted. It is shown in Figure 3. Although this profile was calculated for Camden, March 1980, it is quite similar to that discussed by Budden [1988].

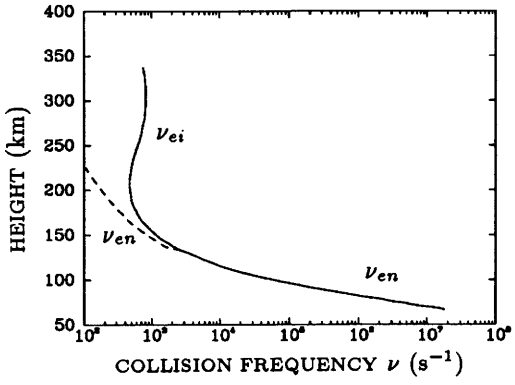

Figure 3: The variation with height of the effective electron-neutral (ν_{en}) and the eletron-ion (ν_{ei}) collision frequencies for Camden, noon, March 1980 (from Ferguson and McNamara [1985]).

The collision frequency profile is employed in tabular form, as listed in Table 2. Values start at 70

Table 2: The collision frequency data for Camden, noon, March 1980, taken from Figure 3.

h(km)	ν(MHz)
70.0	8.547
80.0	1.299
90.0	0.262
100.0	0.063
110.0	0.0169

kilometers, and a constant value is taken above 300 kilometers altitude. The ionosphere is divided into height segments according to the table, and for each segment, the average collision frequency is used in the same way as in the Jones Ray Tracing Program [Jones 1968]. It is calculated by linear interpolation using the collision frequency profile expressed in Table 2. Thus the calculation of absorption is handled the same way in the numerical and analytic cases, facilitating a direct comparison of the results.

3.3 Magnetic field model

The earth's magnetic field can be approximated by an earth centered dipole and this is an adequate representation for our purpose. According to this approximation, e.g. [Davies 1969], the magnetic dip I, is given by

$$\tan I = 2 \tan \Phi \tag{33}$$

where Φ is dipole latitude.

The dipole latitude can be related to geographic coordinate [Davies 1969], but in this study it is convenient to regard the spherical coordinates used to write the ray equations as dipole coordinates. Thus, Φ is the complement of the co-latitude θ. The dip angle is positive in the northern hemisphere, and negative in the southern hemisphere.

In such a model of the earth's magnetic field, the gyrofrequency of electrons at a point (r, Φ) can be expressed as [Davies 1969]

$$f_H = f_{H0}(\frac{r_0}{r})^3 \sqrt{1 + 3\sin^2 \Phi} \tag{34}$$

where

f_H is the electron gyrofrequency,
f_{H0} is the gyrofrequency at the magnetic equator,
r_0 is the earth's radius, and
r is the radial distance from the centre of the earth.

4. Analytic ray tracing results

At the frequencies considered in this study, the exponential D layer included in the model has no significant effect except in the case of absorption. If absorption is not of interest, it may be omitted and this will greatly speed the calculations. However, for completeness the following results include the effect of the D layer. Since refraction in this region is slight, it is treated as a number of uniform spherical slabs, each with the average properties of the height range making up the slab.

In the following discussion, absorption is treated separately.

4.1 No field results

When the earth's magnetic field is ignored, the group path, P', the ground range measured along the earth's surface, D, and the phase path P are given in (22), (24) and (23). With our defined ionospheric model, these equations can be expressed further as

$$\begin{aligned} P' &= 2\Big(\int_{r_0}^{r_d} \frac{r\,dr}{\sqrt{r^2 - r_0^2\cos^2\beta_0}} + \int_{r_d}^{r_{MD}} \frac{r\,dr}{\sqrt{r^2\mu^2 - r_0^2\cos^2\beta_0}} + \int_{r_{MD}}^{r_t} \frac{r\,dr}{\sqrt{Ar^2 + Br + C}}\Big) \\ &= P'_0 + P'_D + P'_E \end{aligned} \tag{35}$$

$$\begin{aligned} D &= 2r_0^2\cos\beta_0\Big(\int_{r_0}^{r_d} \frac{dr}{r\sqrt{r^2 - r_0^2\cos^2\beta_0}} + \int_{r_d}^{r_{MD}} \frac{dr}{r\sqrt{r^2\mu^2 - r_0^2\cos^2\beta_0}} + \int_{r_{MD}}^{r_t} \frac{dr}{r\sqrt{Ar^2 + Br + C}}\Big) \\ &= D_0 + D_D + D_E \end{aligned} \tag{36}$$

$$P = 2\Big(\int_{r_0}^{r_d} \frac{r\,dr}{\sqrt{r^2 - r_0^2\cos^2\beta_0}} + \int_{r_d}^{r_{MD}} \frac{r\,\mu^2\,dr}{\sqrt{r^2\mu^2 - r_0^2\cos^2\beta_0}} + \int_{r_{MD}}^{r_t} \frac{[(1-C/f^2)r - A/f_2\,\frac{1}{r} - B/f^2]\,dr}{\sqrt{\mathcal{A}r^2 + \mathcal{B}r + \mathcal{C}}}\Big)$$

$$= P_0 + P_D + P_E \qquad (37)$$

The subscripts 0, D and E represent the propagation in free space, in the D region and in the E layer respectively, and

$$\left.\begin{aligned} \mathcal{A} &= 1 - C/f^2 \\ \mathcal{B} &= -B/f^2 \\ \mathcal{C} &= -r_0^2\cos^2\beta_0 - A/f^2 \end{aligned}\right\} \qquad (38)$$

where A, B and C are the parameters of the QPS model.

In the D region, because the square of the plasma frequency is an exponential function and there is no closed form for the second integrals in (35), (36) and (37), the average plasma frequency squared value is used for each small segment in this region.

The detailed results of all the integrals are shown below

$$P_0' = 2(\sqrt{r_d^2 - r_0^2\cos^2\beta_0} - r_0\sin\beta_0) \qquad (39)$$

$$P_D' = \frac{2}{\mu_a^2}\left(\sqrt{r_{MD}^2\mu_a^2 - r_0^2\cos^2\beta_0} - \sqrt{r_d^2\mu_a^2 - r_0^2\cos^2\beta_0}\right) \qquad (40)$$

$$P_E' = 2\sum_{i=1}^{1\text{ or }2}(U_i' - L_i') \qquad (41)$$

$$D_0 = 2r_0[\arccos(\frac{r_0}{r_d}\cos\beta_0) - \beta_0] \qquad (42)$$

$$D_D = 2r_0[\arccos(\frac{r_0\cos\beta_0}{r_{MD}\mu_a}) - \arccos(\frac{r_0\cos\beta_0}{r_d\mu_a})] \qquad (43)$$

$$D_E = 2r_0^2\cos\beta_0\sum_{i=1}^{1\text{ or }2}(U_i - L_i) \qquad (44)$$

$$P_0 = 2(\sqrt{r_d^2 - r_0^2\cos^2\beta_0} - r_0\sin\beta_0) \qquad (45)$$

$$P_D = 2\left(\sqrt{r_{MD}^2\mu_a^2 - r_0^2\cos^2\beta_0} - \sqrt{r_d^2\mu_a^2 - r_0^2\cos^2\beta_0}\right) \qquad (46)$$

$$P_E = 2\sum_{i=1}^{1\text{ or }2}[(1 - \frac{C_i}{f^2})(U_i' - L_i')] + 2\sum_{i=1}^{1\text{ or }2}[(-\frac{A_i}{f^2})(U_i - L_i)] + 2\sum_{i=1}^{1\text{ or }2}[(-\frac{B_i}{f^2})(U_i'' - L_i'')] \qquad (47)$$

where

r_d is the radial distance to the base of the D region, in this case, $r_d = r_0 + 50$,
μ_a is the average refractive index for each small segment in the D region,
U_i', L_i', U_i, L_i and U_i'', L_i'' are values of the last integrals in (35), (36) and (37), evaluated at the upper and lower boundaries of the first and/or then the second segment. Within the segment in which reflection takes place, U_i', U_i and U_i'' are the values at the reflection point, where

$$L_i', U_i' = \begin{cases} \frac{\sqrt{\mathcal{A}_i r^2 + \mathcal{B}_i r + \mathcal{C}_i}}{\mathcal{A}_i} - \frac{\mathcal{B}_i}{2\mathcal{A}_i^{3/2}}\ln[2\sqrt{\mathcal{A}_i(\mathcal{A}_i r^2 + \mathcal{B}_i r + \mathcal{C}_i)} + 2\mathcal{A}_i r + \mathcal{B}_i] & \text{if } \mathcal{A}_i > 0 \\ \frac{\sqrt{\mathcal{A}_i r^2 + \mathcal{B}_i r + \mathcal{C}_i}}{\mathcal{A}_i} - \frac{\mathcal{B}_i}{2(-\mathcal{A}_i)^{3/2}}\arcsin(\frac{2\mathcal{A}_i r + \mathcal{B}_i}{\sqrt{\mathcal{B}_i^2 - 4\mathcal{A}_i\mathcal{C}_i}}) & \text{if } \mathcal{A}_i < 0 \end{cases} \qquad (48)$$

$$U_i, L_i = \begin{cases} -\frac{1}{\sqrt{C_i}} \ln \frac{2\sqrt{C_i(A_i r^2+B_i r+C_i)}+B_i r+2C_i}{r} & \text{if } C_i > 0 \\ \frac{1}{\sqrt{-C_i}} \arcsin \frac{B_i r+2C_i}{\sqrt{B_i^2-4A_i C_i}} & \text{if } C_i < 0 \end{cases} \quad (49)$$

$$L_i'', U_i'' = \begin{cases} \frac{1}{\sqrt{A_i}} \ln[2\sqrt{A_i(A_i r^2 + B_i r + C_i)}+ \\ \qquad 2A_i r + B_i] & \text{if } A_i > 0 \\ \frac{1}{\sqrt{-A_i}} \arcsin\left(\frac{-2A_i r-B_i}{\sqrt{B_i^2-4A_i C_i}}\right) & \text{if } A_i < 0 \end{cases} \quad (50)$$

At the point of reflection, the radical equals zero, then

$$U_n' = \begin{cases} -\frac{B_n}{4A_n^{3/2}} \ln(B_n^2 - 4A_n C_n) & \text{if } A_n > 0 \\ \frac{\pi B_n}{4(-A_n)^{3/2}} & \text{if } A_n < 0 \end{cases} \quad (51)$$

$$U_n = \begin{cases} -\frac{1}{\sqrt{C_n}} \ln \sqrt{B_n^2 - 4A_n C_n} & \text{if } C_n > 0 \\ \frac{\pi}{2\sqrt{-C_n}} & \text{if } C_n < 0 \end{cases} \quad (52)$$

$$U_n'' = \begin{cases} \frac{1}{\sqrt{A_n}} \ln(B_n^2 - 4A_n C_n) & \text{if } A_n > 0 \\ \frac{\pi}{2\sqrt{-A_n}} & \text{if } A_n < 0 \end{cases} \quad (53)$$

In the quasi-parabolic function for the joining layer, A is positive, causing A_1 and C_1 to be negative, so the bottom equations (48), (49) and (50) are used for L_1', L_1 and L_1'' when the ray is propagated through this layer. If the reflection happens within this layer, the bottom equations in (51), (52) and (53) are used as the values for U_1', U_1 and U_1''. If the ray penetrates this joining layer and then is reflected by the E layer, the integration will continue to the upper layer. In this layer, A in the QP function is negative, so that A_2 and C_2 will be positive, and therefore the top equations in (48), (49) and (50) are used and the top equations in (51), (52) and (53) need also to be used as the upper and lower boundaries for this layer.

4.2 With the earth's magnetic field

From the appendix, the effective frequency, as defined there, is given by

$$\frac{\delta f_e}{f} = \frac{1}{2} Y h,$$

so that

$$\begin{aligned} f_e &= f + \delta f_e \\ &= f(1 + \tfrac{1}{2} Y h), \end{aligned} \quad (54)$$

provided Yh is constant in the neighbourhood of the actual ray which exists in the presence of the earth's magnetic field. This is only an approximation to what might be termed the exact equivalent frequency. However, this distinction is not really important in view of the fact that, we can see from Figure 1, the quantity h is varying along the ray path, as is Y. A representative value of h along the ray is used to evaluate the effective frequency, and the method of choosing h is discussed later. In view of the whole series of approximations involved, it is of course more than ever necessary to test the approximate results directly.

It turns out that for the ordinary mode, $\delta f_e \geq 0$, while for the extraordinary mode, $\delta f_e \leq 0$.

Group Path

In the case of the group path, a further correction is required, besides the introduction of the equivalent frequency [Chen *et al.* 1991]. This term essentially arises from the fact that the group path involves a further differentiation or ray variation since

$$P' = P + f \frac{\partial P}{\partial f} \quad (55)$$

where the derivative is taken holding the ray endpoints fixed. The approximate expression becomes [Chen *et al.* 1991]

$$\begin{aligned} P' &= \int (1 - \frac{1}{2} X Y h) du \\ &= P'_{\text{no field}} + \Delta P' \end{aligned} \quad (56)$$

where

u is elapsed group path along the $Y = 0$ ray,

h is the quantity shown in Figure 1,

$X = f_N^2/f_e^2$, (In the calculation of W for the extraordinary mode, $X = f_N^2/f^2$ is used.)
$Y = f_H/f_e$,
$P'_{\text{no field}}$ is the group path for the no field case at the effective frequency, and
$\Delta P'$ is the correction of the group path for the case when the earth's magnetic field is considered.

The quantity h is a very complicated function which depends on X, Y, the local elevation angle of the ray and the magnetic dip angle. In order to obtain a closed form for $\Delta P'$, an average value of h is taken for each segment. Furthermore h is not symmetric about the ray apogee because of different angles between the ray direction and the magnetic field direction for the up going and down going sections of the ray. Hence, the above equation can be further expressed as

$$\Delta P' = -\int_{r_d}^{r_t} \frac{1}{2}(h_{up} + h_{dn}) \frac{X\,Y\,r\,dr}{\sqrt{r^2\mu^2 - r_0^2\cos^2\beta_0}}. \tag{57}$$

In the D region, the average values for both the square of the plasma frequency and quantity h will be taken, then the correction of the group path in this region can be written as

$$\Delta P' = -\frac{1}{2}\frac{f_H}{f_e^3}\int_{r_d}^{r_t} (h_{up} + h_{dn}) \frac{f_{N_a}^2\,r\,dr}{\sqrt{r^2\mu^2 - r_0^2\cos^2\beta_0}}. \tag{58}$$

Within the joining and E layers,

$$\Delta P' = -\frac{1}{2}\frac{f_H}{f_e^3}\int_{r_d}^{r_t} (h_{up}+h_{dn}) \frac{(A/r^2 + B/r + C)r}{\sqrt{Ar^2 + Br + C}} dr. \tag{59}$$

The solutions of all these integrals have already been given in Equation (48)-(53). For the ordinary mode, $\Delta P' \geq 0$, while for the extraordinary mode $\Delta P' \leq 0$.

4.3 Absorption

From (8), the absorption is given by

$$A = \frac{1}{2}\frac{\omega}{c}\int \frac{Z}{(1+g)}\frac{(\mu' - \mu)}{\mu'} du. \tag{60}$$

This equation should be compared with expressions for the phase path

$$P = \int \frac{\mu}{\mu'} du$$

and group path

$$P' = \int du.$$

The quantity g has been discussed earlier in this paper, and is expressed as

$$g = \frac{1}{2}Yh.$$

When the effect of the earth's magnetic field on the absorption is considered, the results can be evaluated approximately along the no-field ray by the frequency scaling technique with the introduction of an additional correction. The approximate equation for absorption becomes [Chen *et al.* 1991]

$$A = \frac{2\pi f_e}{c}\int \frac{Z}{2}\frac{1 - \mu^2 - X\frac{\delta f_e}{f}}{1 + \frac{1}{2}Yh} du \tag{61}$$

which, from (54), can be rewritten as

$$A = \frac{2\pi f_e}{c}\int \frac{Z}{2}\frac{X(1 - \frac{1}{2}Yh)}{1 + \frac{1}{2}Yh} du. \tag{62}$$

The additional correction is closely associated with the additional correction that applies to $P' - P$ and hence to P'. As is the case with group path, the relation between the ordinary and extraordinary mode absorption arises from both the different values of h where it appears explicitly in (62), and from the different effective frequencies. The difference between modes shows the same pattern in each case.

In order to evaluate (62), for each segment average collision frequency and an average value for h are used in the integrand.

4.4 Choice of effective frequency

As mentioned previously, in order to evaluate the effective frequency for each ray, an average value of the quantity h has to be determined first. By the mean value theorem, the average value of h will be that applying at some point on the ray. The situation is complicated by the fact that the best value to be used for h is not the same in all circumstances. Thus the precise selection of this representative point is very difficult. Since h depends upon the angle between the direction of the magnetic field and the wave normal direction (in the absence of the

field, the same as the ray direction), as discussed in Section 2, it depends upon the elevation angle and the magnetic dip angle at a point on the ray. When a ray is travelling through the ionosphere, it's local elevation changes gradually, becoming horizontal at the reflection point. The rate of change of elevation is slow low in the ionosphere but is more rapid near the reflection level. One thing that should be noticed is that the angle between the ray direction and the magnetic field direction is different for up going and down going rays, and this difference becomes larger when the transmitter is placed far away from the magnetic equator with the transmission in the magnetic meridian.

In this work, for the purpose of evaluating the effective frequency, h is evaluated for the ray that exists in the absence of the magnetic field, at the radial distance, r_a, given by the empirical formula

$$r_a = r_b + 0.7 \times (r_t - r_b) \qquad (63)$$

where

> r_b is the radial distance at the base ionosphere, (if the D region is included, r_b is the radial distance at the joining point between the D and the E layers), and
> r_t is the radial distance at the reflection point of the ray.

The quantity h is calculated separately for the up going and down going rays, and the average of these two values used to evaluated the effective frequency.

Some consequences of this choice will emerge when the numerical evaluation of the approximation in the next section.

Once the effective frequency has been determined, the ray tracing procedure is started again at the effective frequency. For each segment of the ray, and separately for the up going and down going sections of the ray, the value of h at the mid point of the segment is calculated for use in the calculation of group path and absorption.

5. Comparison between the Analytical Method and the Numerical Method

In this section, we present some results of the comparison between the results of the analytical and numerical ray tracing methods for several ray parameters such as ground range, group path, phase path and absorption. The numerical results were obtained using a general ray tracing program [Court 1981] based on the widely used Jones [1966] ionospheric ray tracing program. The basic single step relative error was set to 1 in 10^{-4}. With only minor exceptions (discussed later), differences between analytic and numerical results represent errors arising because of the approximate method of including magneto-ionic effects in the analytic method. The errors incurred in using the approximation represented by the analytic method will also be shown.

A systematic study was carried out, for the four integral quantities described, as a function of elevation angle, as indicated schematically in Figure 4. That is, three representative transmitter locations were considered and Northward, Southward and East-West propagation considered. (No additional information, except for a check on symmetry, is gained in considering Southward propagation for a transmitter at the magnetic equator.)

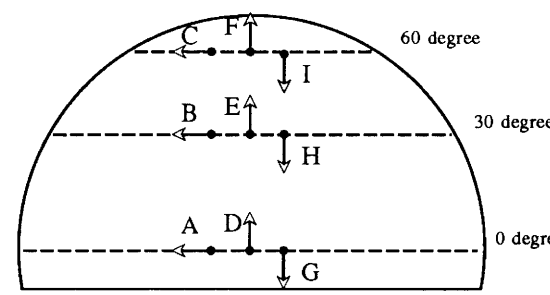

Figure 4: Schematic indication of the transmitter locations and propagation directions considered.

In each case in the comparison, rays at four different frequencies, 2MHz, 3MHz, 4MHz and 5MHz, have been traced.

It is not possible to present all the results here. However, a selection is sufficient to indicate general trends.

This study also allowed a direct comparison of CPU time required by the analytic and numeric ray tracing methods. This comparison was made on a DEC VAX/VMS 8800 using FORTRAN 77

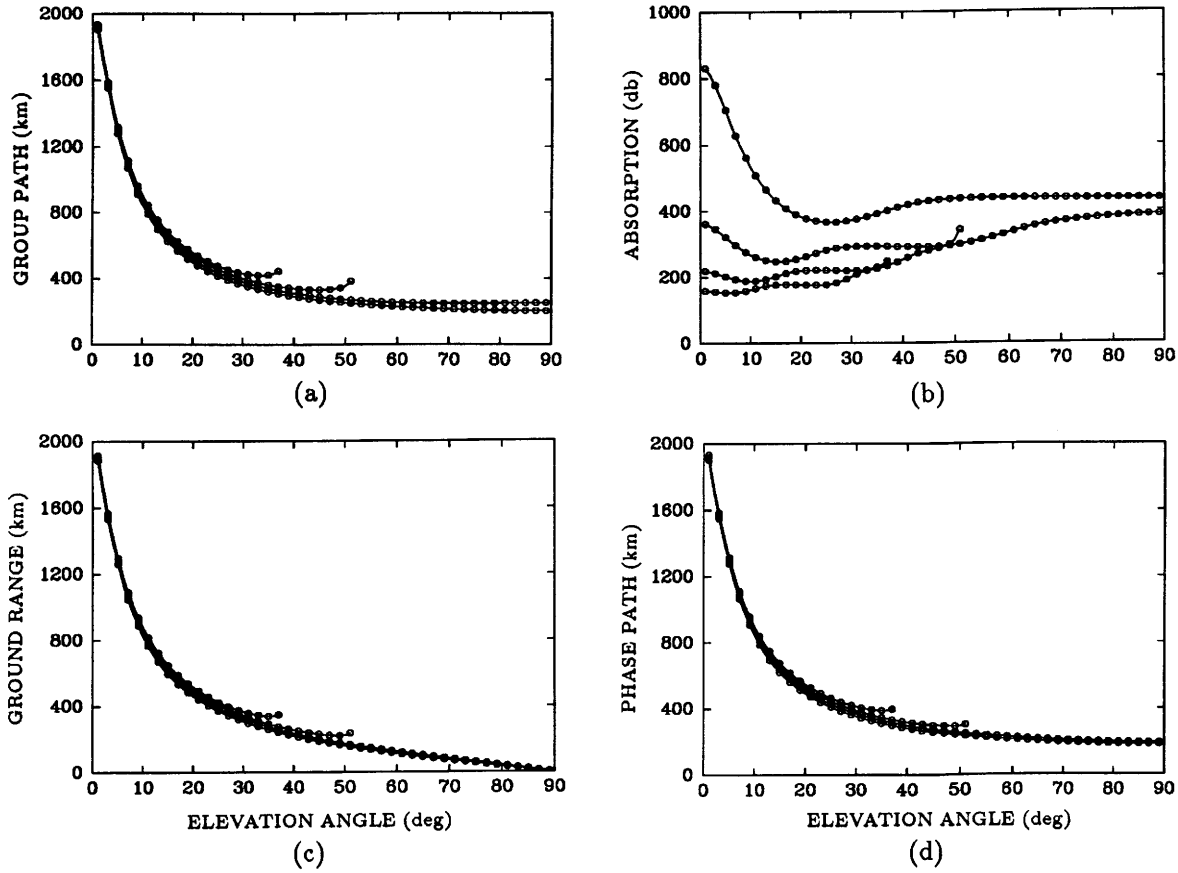

Figure 5: Comparisons between the analytical result and the numerical result for the ordinary mode, for the case in which the propagation is East-West and the transmitter is located at the magnetic equator. The lines represent the analytical result and the dots represent the numerical result. (a) Group path; (b) absorption; (c) ground range; (d) phase path.

programs and the same ionospheric model and initial ray parameters for each program. For numeric tracing, speed depends on the single step error demanded and the complexity of the ionospheric structure. Averaged over the cases considered, it was found that the analytic method requires approximately one fifth the time and if the D layer is omitted, approximately one tenth of the time, required for numerical ray tracing, clearly indicating the advantage of using analytical ray tracing wherever possible.

East-West Propagation at the Equator (A)

This case is presented as a starting point, not because it is typical, but because in this case the no field result applies exactly to the ordinary mode. This can be seen from the graphs of h in Figure 1. Since the propagation is everywhere orthogonal to the magnetic field, h is zero for the ordinary mode, and consequently δf_e is also zero.

Figures 5(a), (b), (c) and (d) show the comparisons for absorption, group path, ground range and phase path for the ordinary mode. Figure 6(a), (b), (c) and (d) show the comparisons for absorption, group path, ground range and phase path for the extraordinary mode. In these figures, the dots represent the results obtained by the numerical method, while the lines represents the results by the analytical method.

Northward Propagation at the Equator (D)

In this case, only error curves are presented. For the group path, the error for the ordinary mode is

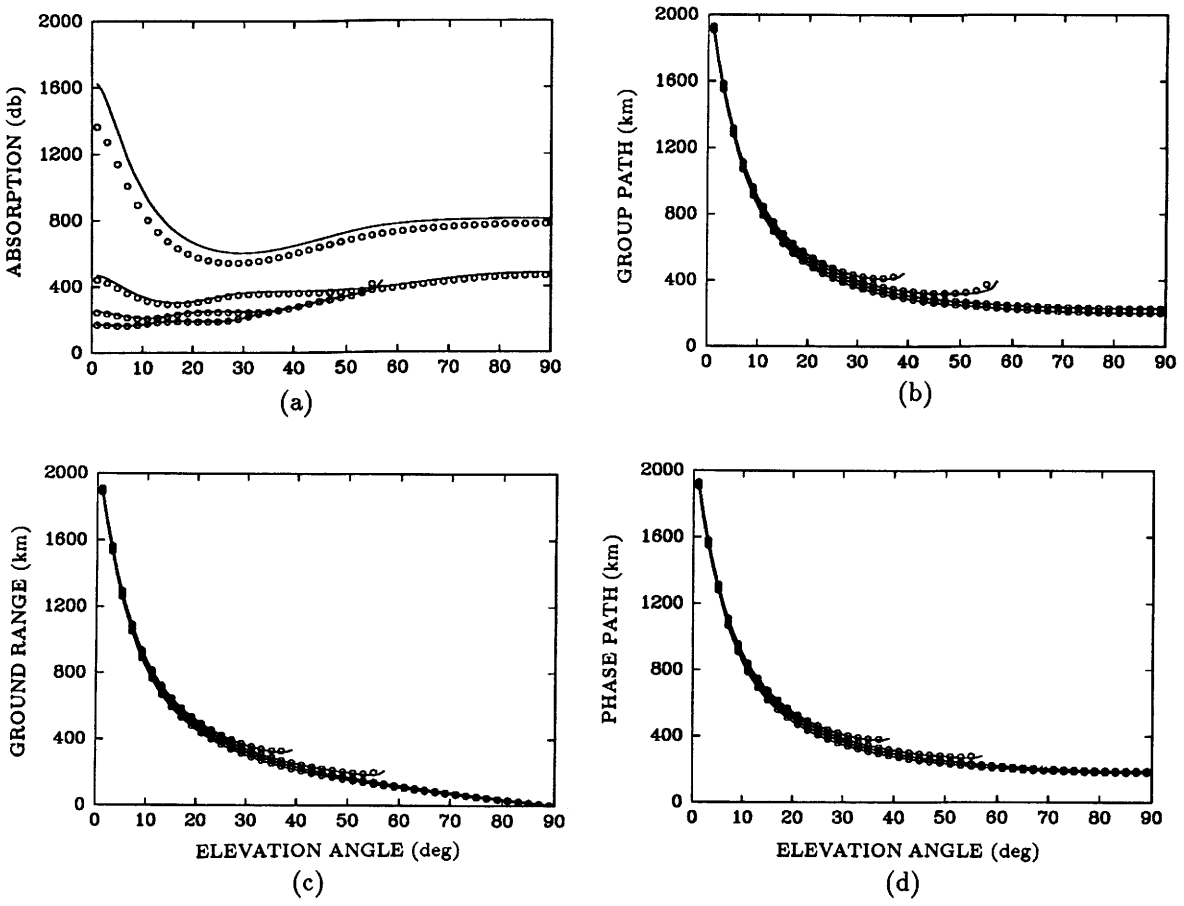

Figure 6: Comparisons between the analytical result and the numerical result for the extraordinary mode, for the case in which the propagation is East-West and the transmitter is located at the magnetic equator. The lines represent the analytical result and the dots represent the numerical result. (a) Absorption; (b) group path; (c) ground range; (d) phase path.

shown in Figure 7(a). The small notch which occurs near 80° elevation in the error curve with the frequency of 2MHz is associated with the phenomenon of the spitze and critical coupling [Budden 1966]. It is not truly an error in the approximation, but a failure of the numerical technique in this situation, where simple ray theory is in any case not valid. The error in the 4MHz curve at higher angles arises from the choice of representative point in the calculation of h. At 90° elevation $h = 0$ for the whole ray. At high elevations, reflection occurs at $X = 1$ where $h = 0$. Since, as is suggested by (22), the major contribution to the integral arises near reflection, it would be appropriate to weight the top of the ray more heavily in calculating the effective frequency. This would reduce the error. The choice represented by (63) is a reasonable compromise for a wide range of situations. For the extraordinary mode, Figure 7(b) shows the corresponding results. They show general behaviour quite similar to that of the ordinary mode.

For phase path, the errors are shown in Figure 7(c) and (d). For ground range, the errors are shown in Figure 7(e) and (f). Very similar variation exists in each case. This has the consequence that if, for example, ground range as a function of group path is of interest, in most cases the errors are significantly reduced.

In the case of absorption relative error is shown in Figure 7(g) and (h).

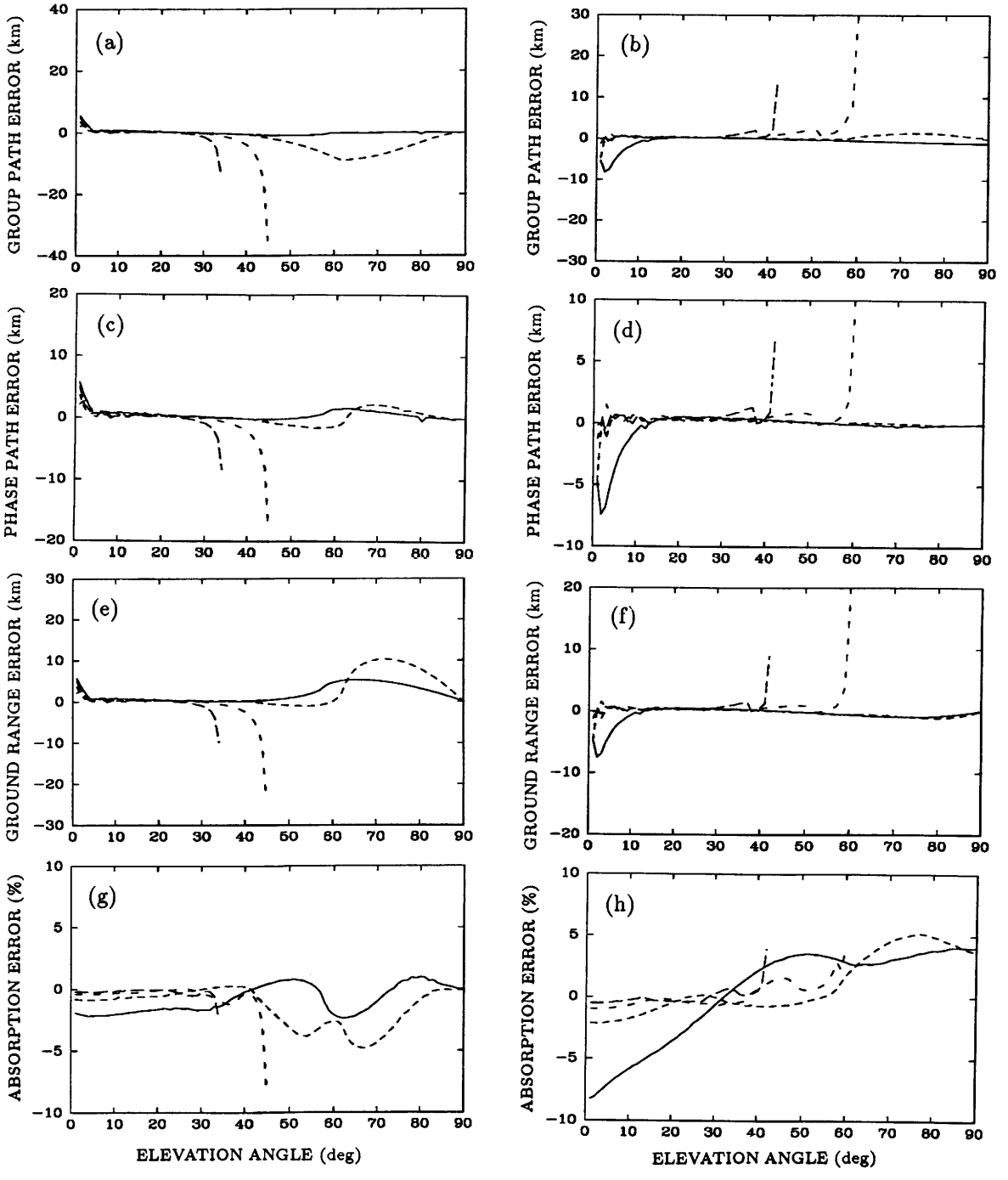

Figure 7: Error curves of the analytical results compared with the numerical results for the case in which the propagation is Northward and the transmitter is located at the magnetic equator. (a) Error for group path for the ordinary mode; (b) error for group path for the extraordinary mode; (c) error for phase path for the ordinary mode; (d) error for phase path for the extraordinary mode; (e) error for ground range for the ordinary mode; (f) error for ground range for the extraordinary mode; (g) relative error for absorption for the ordinary mode; (h) relative error for absorption for the extraordinary mode.

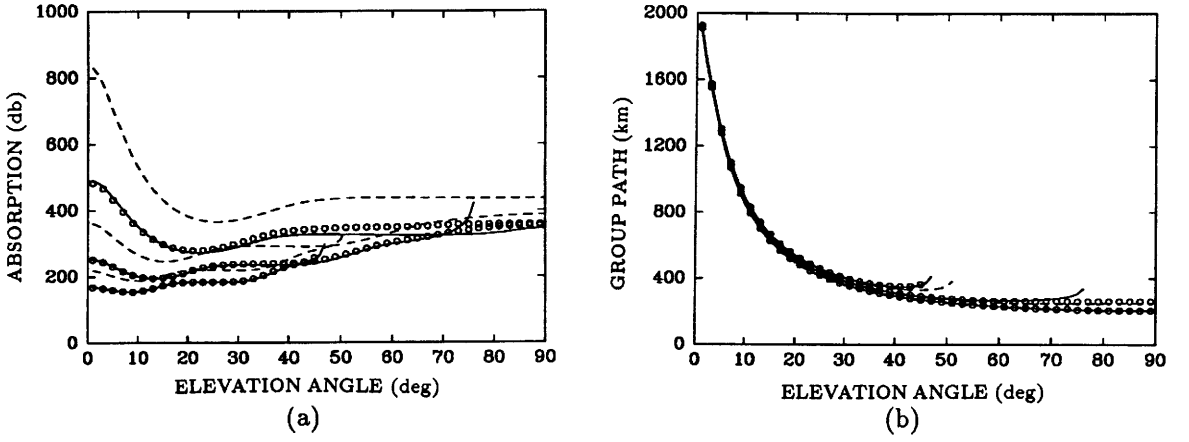

Figure 8: Comparisons between the numerical result, the analytical result and the no field result for the ordinary mode, for the case in which the propagation is in Southward and the transmitter is located at 30° dipole latitude. The dashed lines represent the no field result. (a) Absorption; (b) group path.

Overall Accuracy for Absorption

From all the cases considered, it can be said that the error in calculating absorption is generally between ±10% and frequently between ±5%. Exceptions occur only at very low or very high elevations.

Comparison with No Field Results (H)

Figure 8(a) shows an example of comparison for calculated absorption between the numerical result, the analytical result and the no field result. In this case the propagation is Southward and the transmitter is located at 30° dipole latitude. The dashed line represents the results for no field case. It can be seen that analytic result agrees well with the numerical result. Moreover, it gives much better agreement than simply using the analytic result that applies in the absence of the earth's magnetic field. The influence of the magnetic field on the ordinary mode is greatest on North-South paths lying near the magnetic equator. Figure 8(b) shows an example of similar comparison but concerns group path.

6. Conclusion

It has been shown that analytic formulae for a number of ray quantities describing HF radio propagation in the ionosphere can be extended to take approximate account of the effect of the earth's magnetic field on the propagation.

The ground range and the phase path for both the ordinary and extraordinary modes can be obtained by using the analytic results available neglecting the earth's magnetic field, but using an effective frequency. Results for group path and absorption are obtained using the same equivalent frequencies, but involve also additional correction terms. The results have been compared with the results obtained from the numerical method using a numerical ray tracing program.

The case considered in the comparison cover a wide range of situations. The electron concentration profile is based on actual measurements as represented by the IRI model. Generally, the results obtained from the analytical method agree very well with the results from the numerical method, except at very low frequencies and at certain high angles. Better results could be obtained in the latter case by making a different choice of the representative point on the ray used in the calculation of the equivalent frequency.

The calculations of absorption use the propagation formulae developed by Bennett and Dyson [1978], but extended so that the integration may be taken along rays that exist in the absence of the magnetic field. The method of including the effect of the earth's magnetic field has been shown to be highly accurate. Although the results show unreasonably high absorption in some cases, there

is a good deal of uncertainty about the collision frequency profile which has geographical, diurnal, seasonal and sunspot number dependence.

The advantage of the analytical ray tracing method is its speed. When the ionospheric D region is included, the analytical method is five times faster than the numerical method. If the D region is omitted, the analytical method is ten times faster than the numerical method. This speed advantage is a good reason to employ the analytic approach to ray tracing in many engineering applications of HF ionospheric radio. Only when strong horizontal gradients are present, or in situations in which very detailed studies are required, is there a need to resort to numerical ray tracing.

Appendix: Method of Making Approximate Allowance for the Earth's Magnetic Field

The introduction of a magnetic field greatly complicates the ray tracing. In particular, with the exception of propagation in the magnetic equatorial plane, there are no known cases in which analytic results can be obtained for oblique propagation. The presence of the magnetic field manifests itself through the variable Y, where

$$Y = f_H/f$$

where f is the operating frequency and f_H is the gyrofrequency. Frequency dependence occurs also through X where

$$X = (f_N/f)^2$$

and f_N is the electro-plasma frequency.

Since the rays are characteristics of the eikonal equation, and this equation arises from the characteristic polynomial of a normal matrix, the quantities of interest possess expansions in Y about $Y = 0$ except in special cases. (These cases are associated with singularities in the frequency dependence of elements of the matrix, or caustics of the ray system.) However, the linear term in the expansion vanishes, and the second (quadratic) terms are generally difficult to calculate [Bennett 1973]. We therefore proceed differently.

Consider a typical integral quantity which we write symbolically

$$\mathcal{J} = \int_{ray} i\, du. \qquad (A1)$$

The value of interest is $\mathcal{J}_O$, *i.e.* i and the ray path are evaluated when

$$f = f_O$$

$$f_H = f_{H_O}$$

so that

$$Y = Y_O$$

and

$$\mathcal{J}_O = \int_{ray_O} i_O\, du. \qquad (A2)$$

This is difficult to calculate. If there exists a real point A′ (see Figure A1), *i.e.*

$$f = f_{A'},$$

$$f_H = 0$$

and

$$Y = 0$$

which lies on the contour of constant $\mathcal{J}$ that passes through O then

$$\mathcal{J}_O = \int_{ray_{A'}} i_{A'}\, du. \qquad (A3)$$

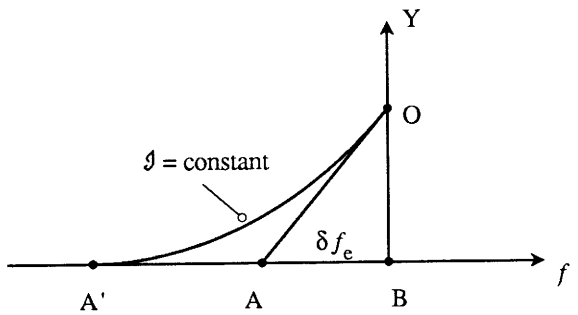

Figure A1: The $Y - f$ plane and the construction used to find δf_e.

Such a point in the (f, Y) plane does not exist in all cases. Even if it does exist, locating it is likely to be no easier than calculating $\mathcal{J}_O$ directly.

Rather than attempting to locate A′, we take a linear approximation to the contour and seek the point A. That is, we wish to find δf_e. Except in exceptional cases, we then have

$$\mathcal{J}_O = \int_{ray_O} i_O\, du = \int_{ray_A} i_A\, du + O(Y_O^2). \qquad (A4)$$

It can be shown that for a number of important integral quantities including ground range and phase path, a single δf_e applies, and is given by

$$\frac{\delta f_e}{f_O} = \frac{1/2Y_O h}{1-1/2Y_O h}, \qquad (A5)$$

provided the right hand side is constant in the neighbourhood of ray_O. In (A4), h is the quantity introduced by Bennett and Dyson [1978] in the discussion of radio wave absorption in the ionosphere.

On the other hand, for a number of other important integrals, including group path and absorption, the required point A is not given by (A5). For such a quantity, say

$$\mathcal{I} = \int_{ray} j\, du. \qquad (A6)$$

rather than attempting to find a different δf_e for these cases, an additional correction is added. It can be shown [Chen *et al.* 1991] that

$$\begin{aligned} \mathcal{I}_O &= \int_{ray_O} j_O\, du \\ &= \int_{ray_A} j_A\, du + \int_{ray_O} \varsigma_O X_O Y_O\, du + O(Y_O^2) \end{aligned} \qquad (A7)$$

provided the condition stated below (A5) is satisfied. The coefficient ς_O proves to be very complicated. However, when evaluated for $Y = 0$, it turns out for the two cases mentioned that for all rays ς_A is a constant independent of frequency.

The whole purpose of our analysis is to avoid having to find the ray_O. If the additional correction term is evaluated along ray_A a result of the same order is obtained. Thus

$$\begin{aligned} \mathcal{I}_O &= \int_{ray_O} j_O\, du \\ &= \int_{ray_A} j_A\, du + \int_{ray_A} \varsigma_A X_A Y_A\, du + O(Y_O^2). \end{aligned} \qquad (A8)$$

It makes little difference whether Y_A or Y_O is used in the correction term. It is not immediately obvious if better numerical results will be obtained by using X_A or X_O.

As pointed out in the text, the right hand side of (A5) does not strictly satisfy the necessary condition for most situations of interest. However, it is found that numerically useful results are obtained by taking a representative value of h. Since, the whole point is to avoid having to find ray_O, in practice the best that can be done is to chose the representative value making use of ray_A. Since initially, δf_e is not known, it is necessary to either evaluate h along ray_B or determine δf_e iteratively.

Acknowledgements

This work has been supported by the Electronics Research Laboratory and the Surveillance Research Laboratories of the Defence Science and Technology Organisation.

Reference

Appleton, E.V. (1928) Some notes on wireless methods of investigating the electrical structure of the upper atmosphere, 1, *Proc. Phys. Soc. London*, **41**, *43-59.*

Baker, D.C. and S. Lambert (1989) Range estimation for SSL HFDF systems by means of a multiquasiparabolic ionospheric model, *IEE Proceedings*, **H 136**, *120-125.*

Bennett, J.A. (1973) Variations of the ray path and phase path: A Hamiltonian formulation, *Radio Sci.* **8**, *737-744.*

Bennett, J.A. and P.L. Dyson (1978) On the relationship between phase path, group path and attenuation in a cold plasma, *J. Plasma Phys.*, **19**, *325-348.*

Bennett, J.A. and P.L. Dyson (1990) Advances in ionospheric ray tracing, *Proceedings Solar Terrestrial Predictions Workshop, 1989, Leura, Australia, NOAA, Boulder U.S.A.*, **1**, *46-52.*

Booker, H.G. (1936) Oblique propagation of electromagnetic waves in a slowly varying non-isotropic medium, *Proc. Roy. Soc.* **A**, **155**, *235.*

Budden, K.G. (1966) Radio waves in the ionosphere, *Cambridge University Press.*

Budden, K.G. (1988) The propagation of radio waves, *Cambridge University Press.*

Chen, J., J.A. Bennett and P.L. Dyson (1990) Automatic fitting of quasi-parabolic segments to ionospheric profiles with application to ground range estimation for single-station location, *J. Atmos. Terr. Phys.* **52**, *277-288.*

Chen, J., J.A. Bennett and P.L. Dyson (1991) Synthesis of oblique ionograms from vertical ionograms by using QPS ionospheric model, *submitted to J. Atmos. Terr. Phys..*

Croft, T.A. and H. Hoogasian (1968) Exact ray calculations in quasi-parabolic ionosphere, *Radio Sci.* **3**, *69-74.*

Conway, A.W. and J.L. Synge (1931) Eds. The mathematical papers of Sir William Rowan Hamilton, **1**, *Geometrical Optics, 164-293, Cambridge University Press, London.*

Davies, K. (1969) Ionospheric radio waves, *Blaisdell Publishing Company (A DIVISION OF GINN AND COMPANY).*

Dyson, P.L. and J.A. Bennett (1980) A universal chart for use in relating ionospheric absorption to phase path and group path, *Trans. IEEE. Antennas Propagn.* **AP-28**, *380-384.*

Dyson, P.L. and J.A. Bennett (1988) A model of the vertical distribution of the electron concentration in the ionosphere and its application to oblique propagation studies, *J. Atmos. Terr. Phys.* **50**, *251-262.*

Dyson, P.L. and J.A. Bennett (1991) Exact ray path calculations using realistic ionospheres, *to be published on IEE Proceedings* **H**.

Ferguson, B.G. and L.F. McNamara (1986) Calculation of HF absorption using the International Reference Ionosphere, *J. Atmos. Terr. Phys.* **48**, *41-49.*

Haselgrove, J. (1955) Ray theory and a new method of ray tracing, *Physics of the Ionosphere, 355-364, Physical Society, London.*

Haselgrove, C.B. and J. Haselgrove (1960) Twisted ray paths in the ionosphere, *Proc. Phys. Soc. London,* **75**, *357-363.*

Hill, J.R. (1979) Exact ray paths in a multisegment quasi-parabolic ionosphere, *Radio Sci.* **14**, *855-861.*

Lewis, R.M. (1965) Asymptotic theory of wave propagation, *Arch. Rath. Mech. Anal.,* **20**, *191-250.*

Milsom, J.D. (1985) Exact ray path calculations in a modified Bradley/Dudeney model ionosphere, *IEE Proceedings* **H 132**, *33-38.*

Poeverlein, H. (1948) Strahlwege von Radiowellen in der Ionosphäre, *S.B. bayer Akad. Wiss. 175.*

Synge, J.L. (1954) Geometrical mechanics and de Broglie waves, *Cambridge University Press, London, 136-144.*

Westover, D.E. (1968) Exact ray-path solutions in a quasi-linear ionosphere, *Radio Sci.* **3**, *75-79.*

Reference is also made to the following unpublished materials:

Court, P.A. (1981) Two ray tracing programs: Software and Manual, *Dept. of Electrical Engineering, Monash University.*

Jones, R.M. (1966) A three-dimensional ray tracing computer program, *ESSA Technical Report IER 17-ITSA 17,* and (1968) Modification to the three-dimensional ray tracing program described in *IER 17-ITSA 17, ERLTM ITS-134.*

Rawer, K. (1981) International Reference Ionosphere - IRI 79, *Rep. UAG-82, National Oceanic and Atmospheric Administration, US Dept. of Commerce, Washington, DC.*